

Linear Free Energy of Activation Relationship for Barrierless Association Reactions

Pascal de Sainte Claire, Gilles H. Peslherbe, Haobin Wang, and William L. Hase*

Contribution from the Department of Chemistry, Wayne State University, Detroit, Michigan 48202-3489

Received April 15, 1996[⊗]

Abstract: An analysis of variational transition state theory rate constants, for the association reactions $\text{Cl}^- + \text{CH}_3\text{Cl}$, $\text{Cl}^- + \text{CH}_3\text{Br}$, $\text{H} + \text{CH}_3$, $\text{H} + \text{diamond}\{111\}$, $\text{CH}_3 + \text{CH}_3$, and $\text{Al} + \text{Al}_2$ shows that the free energy of activation ΔG^\ddagger varies nearly linearly with temperature, over a broad temperature range, for each reaction. This suggests that association rate constants can be parametrized by the free energy of activation at 300 K, ΔG_{300}^\ddagger , and the change in ΔG^\ddagger with temperature, $\Delta\Delta G^\ddagger/\Delta T$. The near linear dependence of ΔG^\ddagger with temperature is supported by a semiempirical model for association kinetics. The rate constants for $\text{Cl}^- + \text{CH}_3\text{Cl}$, $\text{Cl}^- + \text{CH}_3\text{Br}$, and $\text{CH}_3 + \text{CH}_3$ decrease with increase in temperature, while those for $\text{H} + \text{CH}_3$, $\text{H} + \text{diamond}\{111\}$, and $\text{Al} + \text{Al}_2$ slightly increase. For the six association reactions considered here, the linear free energy relationship gives semiquantitative rate constants over a rather broad temperature range of 200–2000 K. To calculate accurate rate constants over a broader temperature range, particularly at low temperatures, nonlinear terms must be included in the free energy expansion.

I. Introduction

A particularly interesting class of reactions are association reactions without a potential energy barrier.¹ These reactions are important for a diverse group of processes such as gas–surface adsorption; ion complexation; radical–radical, radical–molecule, and ion–molecule association; and nucleation and cluster growth. Rate constants for such association reactions can exhibit both positive and negative temperature dependencies, depending on the attractiveness of the radial potential and the anisotropy of the angular potential.² The variational version of transition state theory (TST) has been used to calculate temperature-dependent rate constants for these reactions.^{3–6}

In canonical variational transition state theory (CVTST), the transition state is located at the free energy maximum along the reaction path and the association rate constant is given by

$$k(T) = \frac{k_B T}{h} \exp(-\Delta G^\ddagger/RT) \quad (1)$$

where ΔG^\ddagger is the free energy difference between the variational transition state and the reactants. The temperature-dependent TST rate constant can also be found with use of microcanonical VTST (μCVTST). The microcanonical variational transition state is dependent on total energy E and angular momentum J and is located at the minimum in the sum of states $N^\ddagger(E, J)$ along the reaction path. The association rate constant is then

$$k(T) = \frac{1}{hQ_r} \int_0^\infty \sum_{J=0}^\infty N^\ddagger(E, J) e^{-E/k_B T} dE \quad (2)$$

where Q_r is the reactant partition function. In more detailed versions of μCVTST , the minimum in the transition state sum of states may also depend on the rotational quantum number K for a vibrator transition state⁷ or the orbital angular momentum quantum number L for an orbiting transition state.^{6,8}

Both CVTST and μCVTST association rate constants have been calculated from analytic potential energy functions, often derived in part from *ab initio* calculations.^{9–19} These calculations require determining the reaction path on the potential energy function and properties associated with the reaction path, so that the free energy and sum of states can be determined as a function of the path. Calculations of this type have used either the reaction path Hamiltonian²⁰ or a Hamiltonian based on that for the product fragments.^{6,21,22} Though such calculations give accurate rate constants, they are often rather laborious. There is considerable interest in interpreting such calculated rate

(7) Zhu, L.; Hase, W. L. *Chem. Phys. Lett.* **1990**, 175, 117.

(8) Peslherbe, G. H.; Hase, W. L. *J. Chem. Phys.* **1994**, 101, 8535.

(9) Rai, S. N.; Truhlar, D. G. *J. Chem. Phys.* **1983**, 79, 6046.

(10) (a) Hase, W. L.; Duchovic, R. J. *J. Chem. Phys.* **1985**, 83, 3448.

(b) Hase, W. L.; Mondro, S. L.; Duchovic, R. J.; Hirst, D. M. *J. Am. Chem. Soc.* **1987**, 109, 2916.

(11) Hu, W.; Hase, W. L. *J. Chem. Phys.* **1991**, 95, 8073.

(12) Vande Linde, S. R.; Hase, W. L. *J. Phys. Chem.* **1990**, 94, 2778.

(13) Wang, H.; Zhu, L.; Hase, W. L. *J. Phys. Chem.* **1994**, 98, 1608.

(14) de Sainte Claire, P.; Barbarat, P.; Hase, W. L. *J. Chem. Phys.* **1994**, 101, 2476. Song, K.; de Sainte Claire, P.; Hase, W. L.; Hass, K. C. *Phys. Rev. B* **1995**, 52, 2949.

(15) Yu, J.; Klippenstein, S. J. *J. Phys. Chem.* **1991**, 95, 9882.

Klippenstein, S. J.; East, A. L. L.; Allen, W. D. *J. Chem. Phys.* **1994**, 101, 9198. Klippenstein, S. J.; East, A. L. L.; Allen, W. D. *J. Chem. Phys.* Submitted for publication.

(16) Klippenstein, S. J.; Kress, J. D. *J. Chem. Phys.* **1992**, 96, 8164. Kress, J. D.; Klippenstein, S. J. *Chem. Phys. Lett.* **1992**, 195, 513. Yang, C.-Y.; Klippenstein, S. J.; Kress, J. D.; Pack, R. T.; Parker, G. A.; Lagana, A. J. *Chem. Phys.* **1994**, 100, 4917.

(17) Klippenstein, S. J.; Radivoyevitch, T. *J. Chem. Phys.* **1993**, 99, 3644.

(18) Klippenstein, S. J.; Kim, Y.-W. *J. Chem. Phys.* **1993**, 99, 5790.

(19) Yang, C.-Y.; Klippenstein, S. J. *J. Chem. Phys.* **1995**, 103, 7287.

(20) Miller, W. H.; Handy, N. C.; Adams, J. E. *J. Chem. Phys.* **1980**, 72, 99.

(21) Wardlaw, D. M.; Marcus, R. A. *Adv. Chem. Phys.* **1987**, 70, 231.

(22) Klippenstein, S. J. *J. Phys. Chem.* **1994**, 98, 11459. Klippenstein, S. J. In *Advances in Physical Chemistry: The Chemical Dynamics and Kinetics of Small Radicals*; Liu, K., Wagner, A. F., Eds.; World Scientific: River Edge, NJ, 1995.

[⊗] Abstract published in *Advance ACS Abstracts*, May 1, 1997.

(1) Hase, W. L.; Wardlaw, D. M. In *Bimolecular Collisions*; Ashfold, M. N. R., Baggott, J. E., Eds.; Royal Society of Chemistry: London, 1989; p 171.

(2) Hu, X.; Hase, W. L. *J. Phys. Chem.* **1989**, 93, 6092.

(3) Hase, W. L. *J. Chem. Phys.* **1976**, 64, 2442.

(4) Quack, M.; Troe, J. *Ber. Bunsenges. Phys. Chem.* **1977**, 81, 329.

(5) Truhlar, D. G.; Garrett, B. C. *Acc. Chem. Res.* **1980**, 13, 440.

(6) Chesnavich, W. J.; Bowers, M. T. In *Gas Phase Ion Chemistry*; Bowers, M. T., Ed.; Academic Press: New York, 1979; Vol. 1, pp 119–151.

constants in terms of thermodynamic parameters such as the free energy, enthalpy, and entropy of activation, i.e. ΔG^\ddagger , ΔH^\ddagger , and ΔS^\ddagger .²³ In the work presented here, a semiempirical model is developed for calculating association rate constants and determining their relations to the above thermodynamic parameters.

II. Thermodynamic Activation Parameters

In recent work in our laboratory VTST calculations, based on the reaction path Hamiltonian, have been used to determine rate constants for (1) the ion–molecule association reactions $\text{Cl}^- + \text{CH}_3\text{Cl} \rightarrow \text{Cl}^- \cdots \text{CH}_3\text{Cl}$ ^{12,24} and $\text{Cl}^- + \text{CH}_3\text{Br} \rightarrow \text{Cl}^- \cdots \text{CH}_3\text{Br}$;¹³ (2) the cluster growth reaction $\text{Al} + \text{Al}_2 \rightarrow \text{Al}_3$;⁸ and (3) the radical–radical association reactions $\text{H} + \text{CH}_3 \rightarrow \text{CH}_4$ ^{10,11} and $\text{H} + \text{diamond}\{111\} \rightarrow \text{H-diamond}\{111\}$.¹⁴ Here, diamond{111} represents the {111} surface of diamond with a C-atom terrace radical site. For the two radical–radical associations and $\text{Al} + \text{Al}_2$, association μCVTST and CVTST give values for $k(T)$ which only differ by a few percent, and the CVTST rate constants for these associations are used in the analysis presented here.^{8,11,14} However, for the ion–molecule associations the CVTST rate constant is nearly two times larger than the μCVTST value.¹³ This is because the ion–molecule potential is very long range and, thus, the microcanonical variational transition state is strongly dependent on E and J . The μCVTST rate constants are used for these ion–molecule associations. Thermodynamic activation parameters ΔG^\ddagger , ΔH^\ddagger , and ΔS^\ddagger calculated from the CVTST and μCVTST rate constants, for the above reactions, are summarized in Table 1. These parameters are given for a standard state of 1 mol/L, so that when ΔG^\ddagger is inserted into eq 1 a rate constant in units of $\text{L mol}^{-1} \text{s}^{-1}$ results.

Previous work¹³ has shown that the above μCVTST rate constants for $\text{Cl}^- + \text{CH}_3\text{Br}$ association are nearly identical with those determined by the trajectory capture model based on the ion-dipole/ion-induced dipole potential.²⁵ Thermodynamic activation parameters, calculated from the $\text{Cl}^- + \text{CH}_3\text{Br}$ trajectory capture rate constants, are listed in Table 1. These activation parameters are similar to those determined from the μCVTST rate constants for $\text{Cl}^- + \text{CH}_3\text{Br}$ association.

The temperature-dependent $2\text{CH}_3 \rightarrow \text{C}_2\text{H}_6$ association rate constant has been calculated by using μCVTST and the flexible transition state model.²⁶ Thermodynamic activation parameters determined from these rate constants are also listed in Table 1.

As expected,^{1,12,13,24} the two ion–molecule reactions have similar activation parameters. ΔH^\ddagger is slightly more negative and ΔG^\ddagger slightly smaller for $\text{Cl}^- + \text{CH}_3\text{Cl}$, since the CH_3Cl dipole is larger than that for CH_3Br . The ion–molecule reactions have the smallest ΔG^\ddagger values for a particular temperature. The two radical–radical association reactions, $\text{H} + \text{CH}_3$ and $\text{H} + \text{diamond}\{111\}$, have similar long-range radial potentials, and Table 1 shows they also have similar ΔH^\ddagger values. The ΔG^\ddagger values are smaller for $\text{H} + \text{CH}_3$, because of its larger ΔS^\ddagger values. This is because overall external rotation contributes to $\text{H} + \text{CH}_3$ association, but not to $\text{H} + \text{diamond}\{111\}$.²⁷ For $\text{H} + \text{CH}_3$ association, the external rotation partition function is larger for the variational transition state than for the reactants.

Table 1. Thermodynamic Activation Parameters for Association Reactions^a

T (K)	ΔH^\ddagger	ΔS^\ddagger	ΔG^\ddagger
$\text{Cl}^- + \text{CH}_3\text{Cl} \rightarrow \text{Cl}^- \cdots \text{CH}_3\text{Cl}$, μCVTST , ref 24			
200	-0.894	-6.39	0.383
250	-1.09	-6.83	0.614
300	-1.30	-7.23	0.867
500	-2.21	-8.51	2.05
750	-3.71	-10.10	3.87
1000	-6.59	-12.79	6.20
$\text{Cl}^- + \text{CH}_3\text{Br} \rightarrow \text{Cl}^- \cdots \text{CH}_3\text{Br}$, μCVTST , ref 13			
200	-0.912	-6.71	0.431
250	-1.10	-7.09	0.675
300	-1.30	-7.46	0.942
500	-2.22	-8.78	2.17
750	-3.68	-10.33	4.06
1000	-5.76	-12.12	6.36
$\text{Cl}^- + \text{CH}_3\text{Br} \rightarrow \text{Cl}^- \cdots \text{CH}_3\text{Br}$, trajectory capture, refs 2, 13, 25 ^b			
200	-0.947	-6.83	0.418
250	-1.16	-7.32	0.672
300	-1.38	-7.77	0.951
500	-2.29	-9.09	2.25
750	-3.34	-9.99	4.15
1000	-4.31	-10.53	6.22
$\text{Al} + \text{Al}_2 \rightarrow \text{Al}_3$, CVTST , ref 8			
100	-0.392	-5.95	0.203
150	-0.588	-6.73	0.422
200	-0.787	-7.31	0.674
250	-0.976	-7.71	0.951
300	-1.18	-8.10	1.25
350	-1.38	-8.39	1.56
$\text{H} + \text{CH}_3 \rightarrow \text{CH}_4$, CVTST , ref 11			
300	-1.03	-10.9	2.24
500	-1.60	-11.5	4.14
750	-2.32	-12.0	6.68
1000	-3.80	-13.2	9.42
1500	-5.86	-14.0	15.3
2000	-8.04	-14.8	21.4
$\text{H} + \text{diamond}\{111\} \rightarrow \text{H-diamond}\{111\}$, CVTST , ref 14			
300	-1.36	-16.2	3.49
500	-2.01	-16.8	6.40
750	-2.82	-17.3	10.2
1000	-3.60	-17.6	14.0
1500	-5.28	-18.2	22.1
2000	-7.01	-18.7	30.2
$\text{CH}_3 + \text{CH}_3 \rightarrow \text{C}_2\text{H}_6$, μCVTST , ref 26			
296	-1.29	-14.7	3.05
407	-1.87	-15.7	4.51
474	-2.25	-16.4	5.53
513	-2.48	-16.5	5.97
539	-2.64	-16.7	6.36
577	-2.88	-17.0	6.92
700	-3.66	-17.9	8.86
810	-4.40	-18.6	10.7
906	-5.05	-19.2	12.3
1350	-8.18	-21.1	20.3
1600	-10.07	-22.1	25.3
2000	-13.66	-23.6	33.6

^a ΔH^\ddagger and ΔG^\ddagger are in units of kcal/mol and ΔS^\ddagger is in units of cal/K. Standard state is 1 mol/L. ^b The $\text{Cl}^- + \text{CH}_3\text{Br}$ trajectory capture rate constants were calculated from eq 5 of ref 24a, using a dipole moment of 1.87 D and polarizability of 4.53 Å³.

The thermodynamic parameters are similar for $\text{CH}_3 + \text{CH}_3$ and $\text{H} + \text{diamond}\{111\}$ association, but they have different temperature dependencies.

III. Linear Free Energy Relationship

An interesting result in Table 1 is the near linearity of ΔG^\ddagger versus T for a particular association reaction. This is illustrated in Figure 1 for the ion–molecule and in Figure 2 for the alkyl radical association reactions, respectively. The straight lines

(23) (a) Truhlar, D. G.; Garrett, B. C. *J. Am. Chem. Soc.* **1989**, *111*, 1232. (b) Steinfeld, J. I.; Francisco, J. S.; Hase, W. L. *Chemical Kinetics and Dynamics*; Prentice Hall: New York, 1989; pp 321–323.

(24) Vande Linde, S. R.; Hase, W. L. *J. Chem. Phys.* **1990**, *93*, 7962.

(25) (a) Su, T.; Chesnavich, W. J. *J. Chem. Phys.* **1982**, *76*, 5183. (b) Su, T. *J. Chem. Phys.* **1988**, *88*, 4102.

(26) Wagner, A. F.; Wardlaw, D. M. *J. Phys. Chem.* **1988**, *92*, 2462.

(27) Barbarat, P.; Accary, C.; Hase, W. L. *J. Phys. Chem.* **1993**, *97*, 11706.

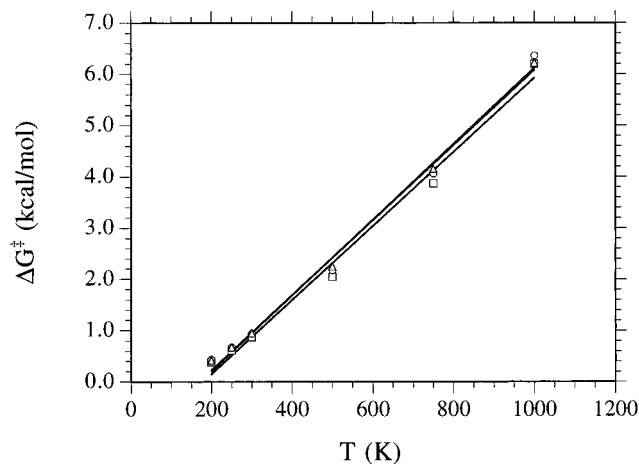


Figure 1. Plot of ΔG^\ddagger versus temperature for $\text{Cl}^- + \text{CH}_3\text{Cl}$, μCVTST (\square); $\text{Cl}^- + \text{CH}_3\text{Br}$, μCVTST (\circ); and $\text{Cl}^- + \text{CH}_3\text{Br}$, trajectory capture (Δ). The ΔG^\ddagger values are from Table 1.

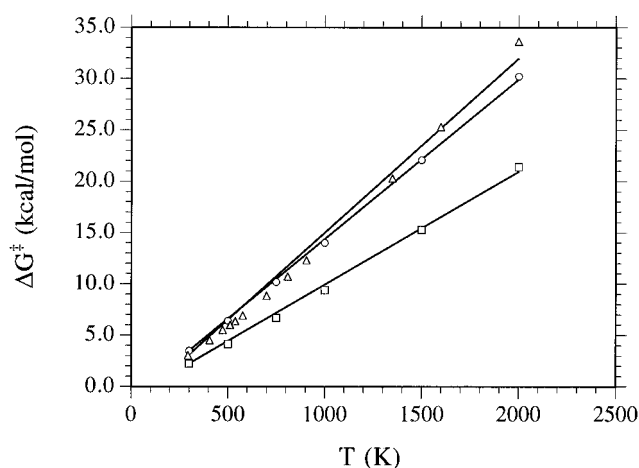


Figure 2. Plot of ΔG^\ddagger versus temperature for $\text{H} + \text{CH}_3$, CVTST (\square); $\text{H} + \text{diamond}\{111\}$, CVTST (\circ); and $\text{CH}_3 + \text{CH}_3$, μCVTST (Δ). The ΔG^\ddagger values are from Table 1.

Table 2. Parameters for the Linear Free Energy Relationship^a

reaction	theoretical method ^b	ΔG^\ddagger_{300} ^c	$\Delta\Delta G^\ddagger/\Delta T$	T range
$\text{Cl}^- + \text{CH}_3\text{Cl}$	μCVTST , ref 24	0.867	0.00722	200–1000
$\text{Cl}^- + \text{CH}_3\text{Br}$	μCVTST , ref 13	0.942	0.00739	200–1000
$\text{Cl}^- + \text{CH}_3\text{Br}$	traj cap., ref 25	0.951	0.00732	200–1000
$\text{Al} + \text{Al}_2$	CVTST , ref 8	1.25	0.00545	100–350
$\text{H} + \text{CH}_3$	CVTST , ref 11	2.24	0.01099	300–2000
$\text{H} + \text{diamond}\{111\}$	CVTST , ref 14	3.49	0.01554	300–2000
$\text{CH}_3 + \text{CH}_3$	μCVTST , ref 26	3.09	0.01698	296–2000

^a ΔG^\ddagger is in units of kcal/mol and T in K. The standard state is 1 mol/L. ^b Theoretical method used to calculate the association rate constants which were then fit to the linear free energy relationship, eq 3. ^c ΔG^\ddagger_{300} is forced to match the calculated values from the theoretical method, given in Table 1.

in these figures are least-squares fits with the free energies of activation at 300 K, ΔG^\ddagger_{300} , forced to match the calculated values in Table 1. Thus, the only fitting parameter for each straight line is the slope $\Delta\Delta G^\ddagger/\Delta T$. The values for ΔG^\ddagger_{300} , and $\Delta\Delta G^\ddagger/\Delta T$ are tabulated in Table 2. From these linear free energy parameters, the free energy versus temperature is

$$\Delta G^\ddagger_T = \Delta G^\ddagger_{300} + (T - 300)\Delta\Delta G^\ddagger/\Delta T \quad (3)$$

and can be used to calculate the association rate constant versus temperature. At 300 K, ΔG^\ddagger is smallest for the ion–molecule associations and largest for $\text{H} + \text{diamond}\{111\}$. There is a

Table 3. Accuracy of the Linear Free Energy Activation Rate Constants

T (K)	rate constants ($10^{10} \text{ L mol}^{-1} \text{ s}^{-1}$)	
	calcd ^a	linear ΔG^\ddagger_T
	$\text{Cl}^- + \text{CH}_3\text{Br}$	
200	146	240
250	135	160
300	127	127
500	108	91.7
750	96.5	90.6
1000	91.1	98.0
	$\text{H} + \text{Diamond}\{111\}$	
300	1.79	1.79
500	1.66	1.37
750	1.69	1.40
1000	1.77	1.53
1500	1.93	1.89
2000	2.06	2.28

^a The calculated rate constants are the trajectory capture values for $\text{Cl}^- + \text{CH}_3\text{Br}$ and CVTST values for $\text{H} + \text{diamond}\{111\}$; see Table 1.

factor of 3 variation in the slope $\Delta\Delta G^\ddagger/\Delta T$ for the different associations.

The accuracy of the association rate constants determined from the linear free energy relation, eq 3, was tested by comparing them with the VTST and trajectory capture rate constants used to derive the ΔG^\ddagger values in Table 1. Overall, the linear free energy relation gives accurate rate constants. This is illustrated in Table 3 where the trajectory capture rate constants for $\text{Cl}^- + \text{CH}_3\text{Br}$ association and CVTST rate constants for $\text{H} + \text{diamond}\{111\}$ are compared with the rate constants determined from the linear free energy relation. For the $\text{H} + \text{diamond}\{111\}$ rate constants, in the range of 300–2000 K, the linear free energy rate constants differ by less than 20% from the CVTST values. For $\text{Cl}^- + \text{CH}_3\text{Br}$ association rate constants in the range of 200–1000 K, the linear free energy and trajectory capture values differ by at most 20% for temperatures between 300 and 1000 K. However, at 200 K the difference becomes nearly 65%.

The increased error in the linear free energy rate constants at low temperatures is because the correct ΔG^\ddagger begin to “level off” as the temperature drops below 300 K and ΔG^\ddagger from the linear free energy relationship becomes too small. The origin of this effect is the loosening of the variational transition state as the temperature is decreased.¹ For an infinitely loose transition state, with properties like those of the reactants, ΔG^\ddagger is zero. The free energy expression could be made more accurate at low temperatures by adding higher order terms, but this would defeat the simplicity of the linear relationship, which gives accurate rate constants over a wide temperature range.

The assumption that ΔG^\ddagger is linear in T , i.e. $\Delta G^\ddagger = a + bT$, yields

$$k(T) = \frac{k_B T}{h} e^{-a/RT} e^{-b/R} \quad (4a)$$

$$= cT e^{-d/T} \quad (4b)$$

when inserted into eq 1. Thus, if association rate constants are fit to the popular form

$$k(T) = BT^n e^{-E/T} \quad (5)$$

one finds that $n \sim 1$. Assuming $n = 0$ yields the Arrhenius expression $k = A \exp(-E_a/RT)$. A shortcoming of this expression is that the A and E_a parameters are strongly

Table 4. Arrhenius Parameters for Association Reactions^a

T (K)	Cl ⁻ + CH ₃ Cl		H + diamond{111}	
	A	E _a	A	E _a
200	1.24	-0.099		
250	1.24	-0.10		
300	1.21	-0.11	0.014	-0.16
750	0.71	-0.73	0.019	0.17
1000	0.25	-2.62	0.021	0.37
1500			0.024	0.68
2000			0.026	0.93

^a A is in units of 10¹² L mol⁻¹ s⁻¹ and E_a in kcal/mol.

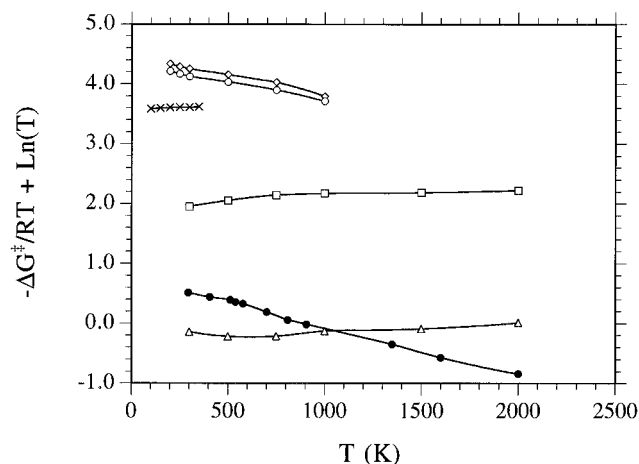


Figure 3. Plot of $[-\Delta G^\ddagger/RT + \ln T]$ to indicate the temperature dependence of $k(T)$. The ΔG^\ddagger values are from Table 1: (\diamond) Cl⁻ + CH₃Cl, μ CVTST; (\circ) Cl⁻ + CH₃Br, μ CVTST; (\times) Al + Al₂, CVTST; (\square) H + CH₃, CVTST; (\triangle) H + diamond{111}, CVTST; and (\bullet) CH₃ + CH₃, μ CVTST.

temperature dependent. This is shown in Table 4 for the fastest and slowest association reactions considered here, i.e. Cl⁻ + CH₃Cl and H + diamond{111}, respectively.

If the association rate constant is cast in the form of eq 1, the variation of the rate constant with temperature is given by

$$\ln(k_2/k_1) = [-\Delta G_2^\ddagger/RT_2 + \ln T_2] - [-\Delta G_1^\ddagger/RT_1 + \ln T_1] \quad (6)$$

The temperature dependence of the rate constant may then be determined from a plot of $(-\Delta G^\ddagger/RT + \ln T)$ versus T . If the slope is zero, k is temperature independent. Negative and positive slopes mean k decreases and increases with T , respectively. The function $-\Delta G^\ddagger/RT + \ln T$ is plotted in Figure 3 for the association reactions considered here. The rate constants for the ion-molecule and CH₃ + CH₃ associations decrease with an increase in T , while those for the remaining associations slightly increase with an increase in T .

IV. Origin of the Linear Free Energy Relationship

A semiempirical model proposed previously^{28,29} may be used to interpret the near linearity of ΔG^\ddagger with temperature. For this model, the free energy as a function of the reaction coordinate r is written as

$$G(r) = G_{\text{vib}}(r) + G_{\text{ir}}(r) + G_{\text{rot}}(r) + V(r) + G_{\text{trans}} + G_{\text{elec}} \quad (7)$$

where the $G_{\text{vib}}(r)$, $G_{\text{ir}}(r)$, and $G_{\text{rot}}(r)$ terms are respectively the free energies for the $3N - 4$ vibrational, internal rotational, and external rotational degrees of freedom orthogonal to the reaction

coordinate and $V(r)$ is the classical potential energy. The free energies for overall translation G_{trans} and the electronic states G_{elec} are assumed to be independent of r . The following assumptions are made to evaluate $G(r)$ for the semiempirical model:

(1) G_{ir} , the free energy for the internal rotation (i.e., torsion) formed during association, is assumed to be constant in the vicinity of the transition state and does not contribute to $dG(r)/dr$. This is an excellent approximation, since this torsion has a small internal rotation barrier and may be modeled as a free rotor. A comparison of methyl rotational barriers for the group of compounds CH₃-M(CH₃)_nH_{3-n}, where M = Si, Ge, Sn, and Pb and $n = 0-3$, suggested that the rotational barrier for the methyl torsion becomes zero for a C-C bond length in the range of 2.2-2.6 Å.³⁰ The C-C bond length is longer at the variational transition state for methyl radical association. In recent work,³¹ an analytic potential energy function derived from high-level *ab initio* calculations was used to determine properties of the variational transition state for CH₃ association with a C-atom radical site on the {111} surface of diamond. The methyl torsion for this transition state was also a free rotor. Note that when an atom associates with a polyatomic radical, a torsion is not formed.

(2) The "pseudo" diatomic approximation³²⁻³⁴ is made to calculate the free energy for external rotation $G_{\text{rot}}(r)$. The moment of inertia for external rotation about the reaction coordinate r is assumed to be constant. The moment of inertia is μr^2 for each of the two remaining degrees of freedom (μ is the reduced mass for the associating fragments).

(3) To evaluate $G_{\text{vib}}(r)$ only the free energies for the "transitional" bending modes,^{1,35} formed as the reactants associate, are assumed to depend on r . For an atom + nonlinear polyatomic association such as Cl⁻ + CH₃Br association there are two transitional bending modes, while for association of two nonlinear polyatomics such as CH₃ + CH₃ there are four transitional bending modes.¹ Tests made in previous work^{1,10b} show that the free energy for a transitional bending mode may be calculated by using the classical partition function $k_B T/h\nu$. Electronic structure theory calculations have been used to determine force constants for transitional bending modes as a function of the distance r between the associating moieties.^{10b,12,14,36} The attenuation of the force constant with change in r has been represented by a hyperbolic tangent function,^{10b,36} and by a sum of terms of the form $a \exp(-br^n)$, where n ranges from 2 to 7.^{12,14} For radical-radical associations this force constant attenuation may be approximated by a Gaussian function.^{2,36,37} The attenuation is more complex for ion-molecule associations.¹² Though the variation of transitional bending mode frequencies with r is not strictly exponential, this has been found to be a very good representation for the limited range of r that encompasses the variational transition state structures for both radical-radical^{10b} and ion-molecule¹² associations. Thus, for the semiempirical model used here, the harmonic vibrational frequency for a transitional bending mode is assumed to vary exponentially with r , in the vicinity of the

(30) Hase, W. L. *J. Chem. Phys.* **1972**, *57*, 730.

(31) de Sainte Claire, P. Ph.D. Thesis, Wayne State University, 1996. de Sainte Claire, P.; Hase, W. L. to be submitted for publication.

(32) Hase, W. L. In *Dynamics of Molecular Collisions*, Part B; Miller, W. H., Ed.; Plenum: New York, 1976; pp 121-169.

(33) Marcus, R. A. *J. Chem. Phys.* **1965**, *43*, 2658.

(34) Bunker, D. L.; Pattengill, M. *J. Chem. Phys.* **1968**, *48*, 772.

(35) Lin, Y. N.; Rabinovitch, B. S. *J. Phys. Chem.* **1970**, *74*, 3151.

(36) Wolf, R. J.; Bhatia, D. S.; Hase, W. L. *Chem. Phys. Lett.* **1986**, *132*, 493.

(37) Truhlar, D. G.; Brown, F. B.; Steckler, R.; Isaacson, A. D. In *The Theory of Chemical Reaction Dynamics*; Clary, D. C., Ed.; D. Reidel: Dordrecht, 1986; pp 285-329.

(28) Hase, W. L. *Chem. Phys. Lett.* **1987**, *139*, 389.

(29) Hase, W. L.; Hu, X. *Chem. Phys. Lett.* **1989**, *156*, 115.

transition state; i.e.

$$v_i(r) = v_i^\circ \exp(-a_i r) \quad (8)$$

Each of the above, i.e., (1)–(3), are excellent approximations for the association reactions considered here.

By making the above assumptions, the free energy versus the reaction coordinate is

$$G(r) = -RT \ln(cT^{3/2}\mu r^2) - RT \sum_{i=1}^m \ln\left(\frac{k_B T}{h\nu_i(r)}\right) + V(r) + G_{ir} + G_{trans} + G_{elec} + G_{vib,con} \quad (9)$$

where c is a constant, m is the number of transitional modes, and $G_{vib,con}$ is the free energy for the $3N - 7 - m$ conserved modes.¹ The frequencies of the conserved modes are assumed to be independent of r . However, it is straightforward to let them vary with r if necessary.^{2,4} The variational transition state is located at the maximum in $G(r)$.^{3–5} After substituting eq 8 for $v_i(r)$, the free energy maximum is found from

$$0 = \frac{dG(r)}{dr} = -RT \left(\frac{2}{r} + \sum_i a_i \right) + \frac{dV(r)}{dr} \quad (10)$$

In the analysis presented here, the situation is treated for which external rotation does not contribute to $G(r)$, as for H + diamond{111} association. For this case, eq 10 becomes

$$0 = \frac{dG(r)}{dr} = -RT \sum_{i=1}^m a_i + dV(r)/dr \quad (11)$$

The long-range potential for an association reaction may be approximated by $V(r) = -b/r^n$. If this expression is inserted into eq 11, the value of r for the variational transition state is found to be

$$r^\ddagger = \left(\frac{nb}{RT \sum_i a_i} \right)^{1/(n+1)} \quad (12)$$

If external rotation contributes to the association rate, the value of r^\ddagger is slightly smaller than that given by eq 12.²⁹

For an association reaction without external rotation, the above model gives for the CVTST rate constant

$$k = \frac{k_B T}{h} e^{-\Delta G^\ddagger/RT} = \frac{k_B T}{h} \frac{Q_{tm}^\ddagger Q_{elec}^\ddagger}{Q_{rel} Q_{elec}} e^{-V(r^\ddagger)/RT} \quad (13)$$

where Q_{tm}^\ddagger and Q_{rel} are the partition functions for the transition state transitional modes and the reactant relative translation, respectively, and $Q_{elec}^\ddagger/Q_{elec}$ is the transition state/reactant electronic partition function ratio. Taking the logarithm of eq 13 gives

$$\Delta G^\ddagger = -RT \left[\sum_{i=1}^m \ln\left(\frac{k_B T}{h\nu_i^\circ}\right) + r^\ddagger \sum_{i=1}^m a_i - \frac{3}{2} \ln\left(\frac{2\pi\mu k_B T}{h^2}\right) + \ln \frac{g^\ddagger}{g_A g_B} - V(r^\ddagger)/RT \right] \quad (14)$$

after inserting the expressions for Q_{tm}^\ddagger , Q_{rel} , and $v_i(r)$, eq 8, assuming the electronic partition function ratio is a ratio of electronic degeneracies, and using a standard state of 1 molecule

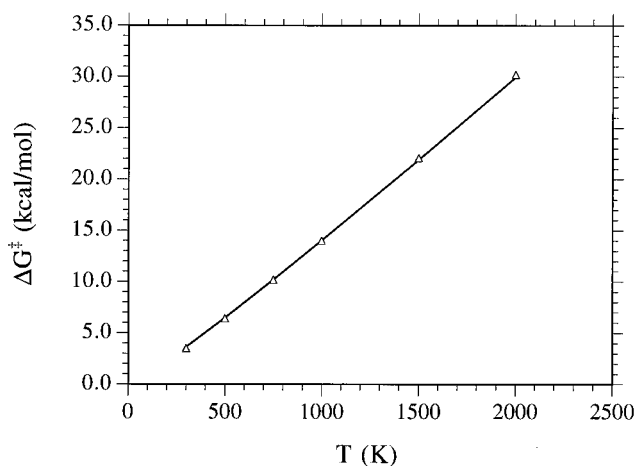


Figure 4. Plot of ΔG^\ddagger versus T , for H + diamond{111} association, determined from CVTST calculations by using the reaction path Hamiltonian, (Δ), and eq 15, solid line.

(atom)/cm³ for Q_{rel} .³⁸ Inserting eq 12 for r^\ddagger into eq 14 and using the long-range attractive potential $-b/r^n$ for $V(r^\ddagger)$ yields

$$\Delta G^\ddagger = -RT \left[\sum_{i=1}^m \ln\left(\frac{k_B T}{h\nu_i^\circ}\right) - \frac{3}{2} \ln\left(\frac{2\pi\mu k_B T}{h^2}\right) + \ln \frac{g^\ddagger}{g_A g_B} + (1 + 1/n) \sum_{i=1}^m a_i \left(\frac{nb}{RT \sum_{i=1}^m a_i} \right)^{1/(n+1)} \right] \quad (15)$$

Since the $\ln T$ and $(1/T)^{1/(n+1)}$ terms in this equation are only weakly dependent on temperature, a plot of ΔG^\ddagger versus T will be nearly linear.

Values of ΔG^\ddagger , for H + diamond{111}, determined from the CVTST calculations (i.e., Table 1) and from eq 15 are compared in Figure 4. The degenerate transitional mode frequency is fit to eq 8 with $\nu^\circ = 30781.761$ cm⁻¹ and $a = 1.677$. The variational transition states for H + diamond{111} have values for r^\ddagger which decrease from 3.32 to 2.69 Å as the temperature is increased from 300 to 2000 K.¹⁴ These ν° and a parameters fit the transitional bending mode frequencies for the transition states¹⁴ to within 3 cm⁻¹. The long-range attractive potential is fit with $b = 13980.189$ kcal·Å⁸/mol and $n = 8$. These parameters fit the 300–2000 K variational transition state potential energies¹⁴ to within 0.1 kcal/mol. The expression $-b/r^n$ also gives accurate transition state potential energies for Al + Al_n → Al_{n+1} association,^{8,39} and is widely used for variational transition states in orbiting transition state/phase space theory⁶ and for ion–molecule associations.⁴⁰ It is seen that eq 15 gives an excellent representation of the CVTST near linear plot of ΔG^\ddagger versus T .

For H-atom association with the diamond{111} surface, external rotation does not contribute to ΔG^\ddagger . For a gas-phase association, external rotation contributes to the transition state free energy and the term

$$-RT \ln[\mu(r^\ddagger)^2/I]$$

where I is the reactant moment of inertia, must be added to eq 14. Since this term is also nearly linear in T , the semiempirical

(38) To convert ΔG^\ddagger to a standard state of one mol/L, $\ln(1000/N_0) = 47.847$ should be added to the terms inside the brackets of the right-hand side of eq 14.

(39) Peslherbe, G. H.; Hase, W. L. *J. Chem. Phys.* **1996**, *105*, 7432.

(40) See for example: Troe, J. *J. Chem. Phys.* **1996**, *105*, 6249.

model provides an explanation for the near-linear plots of ΔG^\ddagger versus T for association reactions.

The presence of the external rotation term for $\text{H} + \text{CH}_3$, but not for $\text{H} + \text{diamond}\{111\}$, is a major reason the $\text{H} + \text{CH}_3$ association rate constant is larger than that for $\text{H} + \text{diamond}\{111\}$.²⁷ As the size of the associating alkyl radical increases, the $\mu(r^\ddagger)^2/I$ term approaches unity and external rotation ceases to contribute to the association rate constant.²⁷

V. Summary

For the six barrierless association reactions considered here it is found that the free energy of activation ΔG^\ddagger is nearly linear with temperature. This result suggests that two parameters, the free energy of activation at 300 K, ΔG_{300}^\ddagger , and the slope of ΔG^\ddagger versus T , $\Delta\Delta G^\ddagger/\Delta T$, can be used to calculate the association rate constant versus temperature. A semiempirical model proposed previously^{28,29} provides an interpretation of the near linearity of ΔG^\ddagger with temperature.

The utility of the linear free energy relationship is that it gives semiquantitative rate constants over a rather broad temperature range, i.e., 200–2000 K for the association reactions considered here. However, the linear free energy relationship does not

correctly represent the $T \rightarrow 0$ and $T \rightarrow \infty$ limits for barrierless association rate constants. To calculate accurate rate constants over a broader temperature range and particularly at low temperatures, nonlinear terms must be included in the free energy expansion. This is an important topic for future study.

The rate constant for an association reaction can either decrease or increase with an increase in temperature. The function $(-\Delta G^\ddagger/RT - \ln T)$ allows one to identify the temperature dependence of the rate constant. It decreases and increases, respectively, if the rate constant decreases and increases with an increase in temperature. The rate constants for the ion-molecule associations $\text{Cl}^- + \text{CH}_3\text{Cl}$, $\text{Cl}^- + \text{CH}_3\text{Br}$, and $\text{CH}_3 + \text{CH}_3$ decrease with increase in temperature, while the rate constants for $\text{Al} + \text{Al}_2$, $\text{H} + \text{CH}_3$, and $\text{H} + \text{diamond}\{111\}$ association slightly increase with an increase in temperature.

Acknowledgment. This research was supported by the National Science Foundation. The authors wish to acknowledge discussions with R. D. Bach which led to the work presented here.

JA961239B